Available online at www.sciencedirect.com
SCIENCE DIRECT®
Journal of Hydrology 300 (2005) 212–233
Journal of Hydrology
www.elsevier.com/locate/jhydrol

New estimates of future changes in extreme rainfall across the UK using regional climate model integrations. 1. Assessment of control climate

H.J. Fowler[a,*], M. Ekström[b], C.G. Kilsby[a], P.D. Jones[b]

[a]*Water Resource Systems Research Laboratory, School of Civil Engineering and Geosciences, University of Newcastle, Cassie Building, Newcastle upon Tyne NE1 7RU, UK*
[b]*Climatic Research Unit, University of East Anglia, Norwich, UK*

Received 8 August 2003; revised 3 June 2004; accepted 3 June 2004

Abstract

Widespread major flood events in both the UK and Europe over the last decade have focussed attention on perceived increases in rainfall intensities. The changing magnitude of such events may have significant impacts upon many sectors, particularly those associated with flooding, water resources and the insurance industry. Here, two methods are used to assess the performance of the HadRM3H model in the simulation of UK extreme rainfall: regional frequency analysis and individual grid box analysis. Both methods use L-moments to derive extreme value distributions of rainfall for 1-, 2-, 5- and 10-day events for both observed data from 204 sites across the UK (1961–1990) and gridded ~50 km by 50 km data from the control climate integration of HadRM3H. Despite differences in spatial resolution between the observed and modelled data, HadRM3H provides a good representation of extreme rainfall at return periods of up to 50 years in most parts of the UK. Although the east–west rainfall gradient tends to be exaggerated, leading to some overestimation of extremes in high elevation western areas and an underestimation in eastern 'rain shadowed' regions, this suggests that the regional climate model will also have skill in predicting how rainfall extremes might change under enhanced greenhouse conditions.

Keywords: Rainfall; Extremes; Climate change; Regional climate models; Floods; UK

1. Introduction

In the past decade, widespread flooding (Marsh, 2001; Lamb, 2001) and landslides (Lawrimore et al., 2001) in the UK and Europe have focussed attention on perceived increases in rainfall intensities. Climate model integrations predict increases in both the frequency and intensity of heavy rainfall in the high latitudes of the Northern Hemisphere under enhanced greenhouse conditions (McGuffie et al., 1999; Jones and Reid, 2001; Palmer and Räisänen, 2002). These projections are consistent with recent increases in rainfall intensity seen in the UK (Osborn et al., 2000;

* Corresponding author. Tel.: +191-222-7113; fax: +191-222-6669.
E-mail address: h.j.fowler@ncl.ac.uk (H.J. Fowler).

0022-1694/$ - see front matter © 2004 Elsevier B.V. All rights reserved.
doi:10.1016/j.jhydrol.2004.06.017

Fowler and Kilsby, 2003a,b), Europe (Brunetti et al., 2000; Frei and Schär, 2001) and worldwide (e.g. Karl and Knight, 1998; Iwashima and Yamamoto, 1993; Zhai et al., 1999), although it is not possible to relate one to the other, as cause and effect.

Changes to the magnitude, character and spatial distribution of extreme rainfall may have serious social and economic implications. Currently, the UK government spends in excess of £300 million annually on flood defences. This is likely to rise by another £200 million when also taking climate change impacts into account (DEFRA, 2001). Recent flood events in the UK in winter 2000/2001 and Europe in summer 2002 produced insurance claims of £1 billion and 19 billion Euros, respectively, and have led the insurance industry in the UK to re-evaluate its position in relation to flooding. Currently, the Association of British Insurers is considering the withdrawal of flood insurance from the 10% of UK properties, worth some £200 billion, considered to have inadequate flood defences after 31st December 2002, and there has been a similar insurance response to flood hazard globally (Crichton, 2002).

Recent extreme rainfall events in the UK have characteristically been multi-day, with unremarkable one-day totals. However, there have been few comprehensive analyses of the current or likely future distribution of multi-day events (e.g. Osborn and Hulme, 2002; Fowler and Kilsby, 2003a,b), with most studies concentrating on daily extremes (e.g. Jones and Reid, 2001; Osborn et al., 2000) or taking a case-study approach (e.g. Huntingford et al., 2003; Lamb, 2001). Regional climate models (RCMs) provide the best information currently available for estimation of changes in extreme rainfall. A study by Jones and Reid (2001) provided the first analysis of future changes in one-day extreme rainfall over the UK. Using results from the HadRM2 RCM (Murphy, 1999), their research suggested dramatic increases in the heaviest rainfall events. However, this model has now been superseded by the HadRM3H integrations, used to produce the new UKCIP02 climate change scenarios for the UK (Hulme et al., 2002).

In this two-part paper, two methods are used to assess the performance of the HadRM3H model in the simulation of UK extreme rainfall and provide new estimates of future change in extreme rainfall across the UK; regional frequency analysis (RFA) and individual grid box analysis (GBA). Both methods derive extreme value distributions of rainfall for 1-, 2-, 5- and 10-day events, fitted using L-moments (Hosking and Wallis, 1997). The RFA involves the regional pooling of annual maxima (AM) and allows a more reliable estimation of high return period rainfall events. The GBA provides additional information on the spatial distribution of extremes. In this paper, the performance of the HadRM3H model is established by comparing return period estimates of extreme rainfall from the control scenario with estimates derived from the previous HadRM2 model and observations. In the second paper (Ekström et al., 2004), results from the HadRM3H model for a future scenario of enhanced greenhouse conditions are examined. This provides both a comparison of future projected changes in extreme rainfall from HadRM2 and HadRM3H models and an indication of how these estimated changes could be used in impact studies. Scenarios derived from HadRM3H are currently the standard in the UK, but will be superseded in due course, and it is therefore useful to assess the differences between model generations.

The application of RFA was pioneered in flood frequency analysis (Hosking and Wallis, 1988; 1997), but has been little used in climate change applications. Return period estimation for extreme rainfall events has commonly been based on single point data series, e.g. Hennessey et al. (1997) and McGuffie et al. (1999). However, RFA provides more robust return period estimates than those estimated using single point data series due to the inclusion of a larger data set. This paper investigates not only the HadRM3H model representation of extreme rainfall in the UK, but also the potential differences in using point estimates, e.g. the GBA, compared to the more comprehensive RFA approach.

2. Data

2.1. Observations

Two observed datasets were used in the study The station data set is that used by Fowler and Kilsby (2003a), comprising 204 stations across the UK with daily rainfall records for the 30-year period 1961–1990. These stations were chosen so that each of

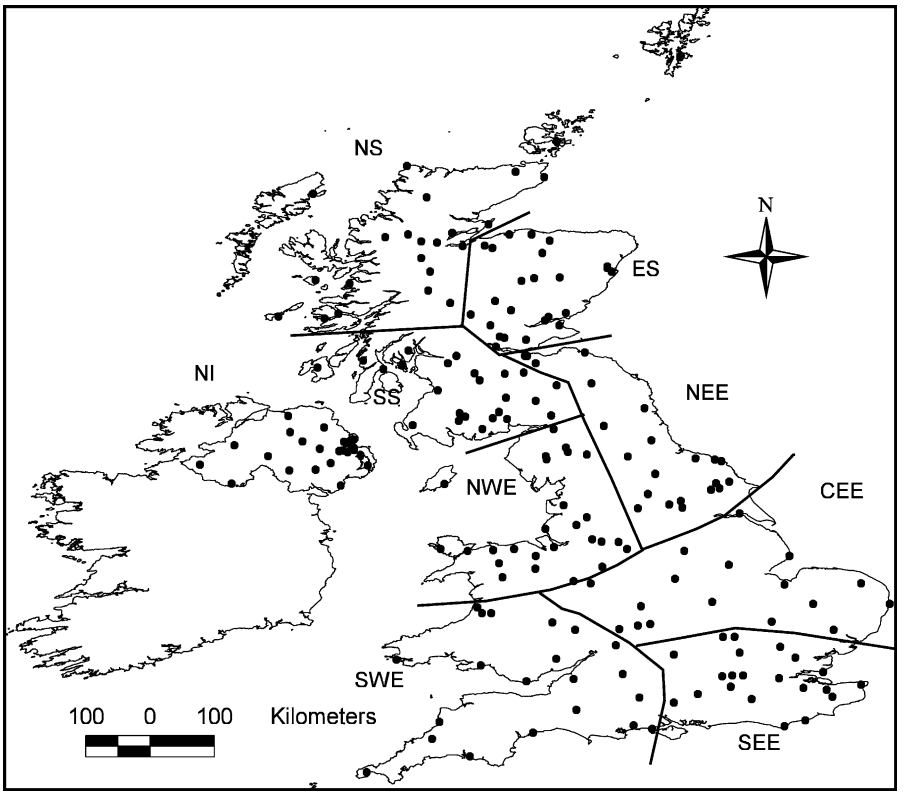

Fig. 1. Location of the 204 UK daily rainfall records with complete or almost complete data for the 1961–2000 period and the nine coherent rainfall regions. The regions are: North Scotland (NS), East Scotland (ES), South Scotland (SS), Northern Ireland (NI), Northwest England (NWE), Northeast England (NEE), Central and Eastern England (CEE), Southeast England (SEE) and Southwest England (SWE) (reproduced with permission from Fowler and Kilsby, 2003a).

the nine spatially coherent rainfall regions for the UK (Wigley et al., 1984; Wigley and Jones, 1987; Gregory et al., 1991; Jones and Conway, 1997) contained at least 20 records (see Fig. 1). The rainfall stations were a compilation of 110 rainfall series used by Osborn et al. (2000) in their study of UK rainfall intensity changes, and subsequently used by Jones and Reid (2001) in their analysis of future changes in UK extreme rainfall estimated by the HadRM2 RCM, and data from the British Atmospheric Data Centre (http://www.badc.rl.ac.uk/).

Additionally, the 5 km gridded dataset developed at the UK Meteorological Office (http://www.metoffice.com/research/hadleycentre/obsdata/ukcip/index.html) was used to provide five-day annual maximum data for each year from 1961 to 1990 for each of the 5 km grid boxes. An explanation of the production of this dataset is given in Appendix 7 of Hulme et al. (2002).

2.2. Models

Two RCM datasets were used in the analysis; HadRM2 and HadRM3H, both developed at the Hadley Centre of the UK Meteorological Office (see Fig. 2). These regional models derive from the HadCM2 (Johns et al., 1997) and HadCM3 (Gordon et al., 2000; Johns et al., 2003) global climate models, respectively. Global climate model (GCM) data are not used in this analysis as the spatial rainfall patterns associated with orography and land-sea differences are not reproduced at their coarse resolution (e.g. HadCM3 grid boxes are $\sim 265 \times 300$ km). Instead we use results from RCMs embedded within GCMs,

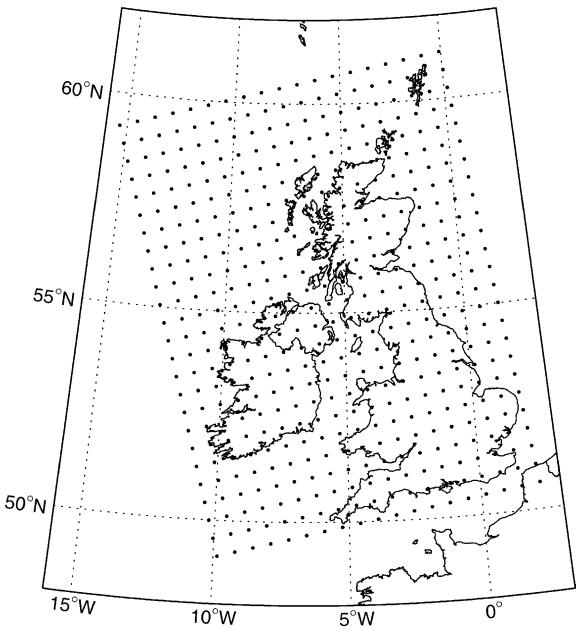

Fig. 2. HadRM3H model dataset over the UK where points denote grid box centres.

which provide finer resolution detail of fine scale weather features.

The HadRM2 model is nested within HadCM2 at a resolution of $\sim 50 \times 50$ km, with integrations conducted using boundary conditions from the HadCM2 model. The HadCM2 integrations used historical levels of greenhouse gases (GHGs) during the period 1860–1990 and a compounding 1% increase in CO_2 for the period 1990–2100, similar to IPCC scenario IS92a (Leggett et al., 1992; Mitchell et al., 1995). Two RCM integrations were then performed. This gave a 30-year control simulation (1961–1990) and a 20-year simulation of increasing GHGs, representing the period 2080–2100 (Murphy, 2000). The integration of HadCM2 used to drive HadRM2 did not include effects of sulphate aerosols, so their effect is omitted.

The HadRM3H integrations represent the current 'state-of-the-art' in climate modelling across Europe and were used to produce the new UKCIP02 climate change scenarios for the UK (Hulme et al., 2002). Boundary conditions are derived from the global atmosphere model, HadAM3H, (Pope et al., 2000) which is of intermediate scale between the coarser resolution HadCM3 and the RCM. The HadAM3H model was run for a reference baseline period (1961–1990). For this run, observed values of sea-surface temperatures (SST) and sea-ice were used instead of their HadCM3 modelled counterpart (Hulme et al., 2002). In the future run (2071–2100), changes in the SST and sea-ice projected by HadCM3 was added to the observations. This method of downscaling gives a more realistic representation of the North Atlantic storm track compared to using a GCM alone (Hulme et al., 2002). Wind, temperature, and humidity output from HadAM3H were then used to run HadRM3H (Hulme et al., 2002).

Seven integrations of the HadRM3H model have been run. Three of these provide an ensemble representation of the control climate period (1960–1990) and the other four represent future climate conditions (2070–2100). Of the future integrations, three form an ensemble based upon the IPCC A2 SRES (Special Report on Emissions Scenarios) 'storyline' (IPCC, 2000) (the UKCIP02 Medium-High Emissions scenario) and the other is based on the B2 SRES 'storyline' which has less severe consequences in terms of climatic change (the UKCIP02 Medium-Low Emissions scenario). The ensemble members involve the same model initiated from three different points in the HadCM3 control run (Hulme et al., 2002). The three ensembles have similar long-term characteristics but show significant year-to-year and decade-to-decade differences due to internal climate variability. These provide a range of potential changes in extreme rainfall across the UK, because the range of outcomes is uncertain.

3. Analysis methods

Two complementary sets of analyses have been undertaken to assess the performance of the HadRM3H model in the simulation of UK extreme rainfall on an annual basis: RFA (Section 3.1) and GBA (Section 3.2). The regional approach allows estimation of the magnitude of long return-period rainfall events with more reliability than single site analyses where only short records are available. The GBA, on the other hand, shows the performance of the RCM at its limited spatial resolution. In both approaches, the analysis was performed using AM of 1-, 2-, 5- and 10-day rainfall totals. Furthermore, both approaches estimate extreme rainfall using

the Generalised Extreme Value (GEV) distribution fitted using the method of L-moments (Hosking and Wallis, 1997) to define extremes with given return periods. Although peak-over-threshold analysis may produce more robust estimates, it was not used here as differences in mean annual rainfall between the observed and RCM datasets would require different threshold values to be used for each simulation.

Estimates of extreme rainfall are expressed here in terms of quantiles. The quantile of a return period (T) is an event magnitude so extreme that it has probability $1/T$ of being exceeded by a single event in any given year (Hosking and Wallis, 1997). The return period can also be seen as the average interval between events of a given magnitude. The 'risk equation' relates the return period (T) to the risk (r) of a design exceedance within a specified number of years (M), where M may be the design lifetime of a structure, i.e.

$$r = 1 - (1 - 1/T)^M \quad (1)$$

More detail on quantile estimation can be found in Palutikof et al. (1999). In this paper we estimate the rainfall amounts associated with 5-, 10-, 25- and 50-year return periods for the RCM control integrations and compare these to observed estimates for the 'common' period 1961–1990. The period is 'common' in the sense that the model is given boundary conditions of the observed SSTs and sea ice distribution together with the measured GHG concentrations. Neither GCM (HadAM3H) nor RCM (HadRM3H) should be expected to reproduce sequences of dry and wet seasons on dates these were actually observed, however, except for the extent to which these are related to SST forcing.

3.1. Regional frequency analysis

The RFA builds on the regionalisation of UK rainfall, first developed by Wigley et al (1984), and later improved and updated by Wigley and Jones (1987), Gregory et al. (1991) and Jones and Conway (1997). This regionalisation identified five spatially coherent regions for England and Wales, three for Scotland and one for Northern Ireland. For each of these regions, a standard RFA approach based on L-moment methods (Hosking and Wallis, 1997) was taken to generate rainfall '*growth curves*' for the rainfall AM data sets. This used the observed dataset 1961–1990 (as Fowler and Kilsby, 2003a), the control scenario from the HadRM2 model and the control ensemble of HadRM3H, comprising three runs each of 31 years.

A growth curve is a standardised extreme value plot of AM. In this study we standardise by Rmed (the median AM rainfall), following the method used in the Flood Estimation Handbook (FEH) (IH, 1999) (detailed in Appendix). For each grid box (for model) and station (for observed), the AM were standardised using the grid box (station) Rmed for that period. L-moment ratios derived from single grid box (station) analyses within a region were then combined by regional averaging and weighted according to record length (after Hosking and Wallis, 1997). A GEV distribution or 'growth curve' was then fitted for each region and aggregation level (1-, 2-, 5- and 10-days) for the RCM (observed) data by matching the sample L-moments to the distribution L-moments. Using these growth curves, the event magnitude for a 5-, 10-, 25- and 50-year return period were estimated for each data set and region using the fitted growth factor multiplied by the regional Rmed. This methodology is explained in more detail in the technical appendix and in Fowler and Kilsby (2003a).

3.2. Grid box analysis

For the GBA, the event magnitude at the 5-, 10-, 25- and 50-year return period were estimated individually per grid box, based on the same L-moment approach as the RFA.

Two approaches may be followed for comparing model grid box extreme rainfall estimates with observed values. The first method is by aggregation, where, for example as in Huntingford et al. (2003), observed daily series from many stations lying within the grid box are spatially averaged to produce a single grid-average daily series. This method is very data intensive, and sufficient data are not available in some parts of the UK. More importantly, the method is not easily applicable in other parts of the world with poorer data provision. Therefore a second, 'down-downscaling', method is used here, where the observed station estimates are modified by an areal reduction factor (ARF) so that they represent

Table 1
Factors for converting Rmed from fixed to sliding duration

Duration (days)	Factor
1	1.16
2	1.11
5	1.035
10	1.005

the equivalent RCM grid box value. The assumptions required by the use of ARFs are discussed later.

This approach is used together with the 'index-flood method', central to RFA, where the standardised growth curves estimated from the RFA are multiplied by a value of Rmed estimated from the UKMO dataset (see Section 2.1) to produce rainfall estimates for the different rainfall durations and the range of return periods that are used here.

The only readily available gridded annual maximum rainfall data were those of the observed UKMO 5 km grids of five-day AM for each year 1961–2000 (see Hulme et al., 2002, their Appendix 7). These were used, as described below, to predict Rmed at 1-, 2- and 10-day duration, using regression relations based on the five-day Rmed, which were derived using the observed daily station data set. Regressions using additional predictors (e.g. SAAR (Standard Annual Average Rainfall, 1961–1990) and location) were investigated but found to give no significant improvement.

Before using it as the predictor in the regression, a grid of Rmed five-day 5 km values was calculated from the annual maximum values for the years 1961–1990.

The site Rmed values for 1961–1990 were based on discrete or fixed duration observations (i.e. 09:00–09:00). It is, however, customary to use sliding duration estimates for design purposes, e.g. allowing for the maximum rainfall observed in any continuous 24-h period irrespective of its actual start and end times. Sliding duration estimates are larger than fixed duration, particularly for smaller durations, so the values were converted using the factors in Table 1. These factors have been interpolated from values used in FEH (IH, 1999) for 1-, 2-, 4- and 8-day durations.

To check that the observed Rmed values were correct and representative, Rmed values corresponding to the daily gauge locations were extracted from the FEH. Good correspondence between site Rmed (1961–1990) and the FEH values was found. This check is, however, limited by the use of records for time periods different to 1961–2000 to form the FEH estimates. The FEH data are generally from 1960 to 1995, with a smaller number of longer records, and the number of records decreasing from 1990 to 1995 (IH, 1999).

Regressions of Rmed for 1-, 2- and 10-day events were carried out on Rmed5 using site Rmed (1961–1990), and the coefficients and results are shown in Table 2. As expected, the regression models explain more variance for longer durations, with the poorest results for one-day duration with r^2 around 0.91. Scatter plots of the regression model values against

Table 2
Regression results: predicting 1-, 2- and 10-day Rmed from 5-day Rmed using station data

Gauge data				
Predictor	Coef	SE Coef	*T*	*P*
One-day RMED = 12.3 + 0.346 five-day RMED				
Constant	12.3381	0.5793	21.30	0.000
Five-day RM	0.345679	0.007864	43.95	0.000
R-Sq = 90.5%; R-Sq(adj) = 90.5%				
Two-day RMED = 9.68 + 0.550 five-day RMED				
Constant	9.6807	0.6251	15.49	0.000
Five-day RM	0.549582	0.008486	64.77	0.000
R-Sq = 95.4%; R-Sq(adj) = 95.4%				
Ten-day RMED = −12.9 + 1.60 five-day RMED				
Constant	−12.880	1.167	−11.03	0.000
Five-day RM	1.59930	0.01585	100.93	0.000
R-Sq = 98.1%; R-Sq(adj) = 98.0%				

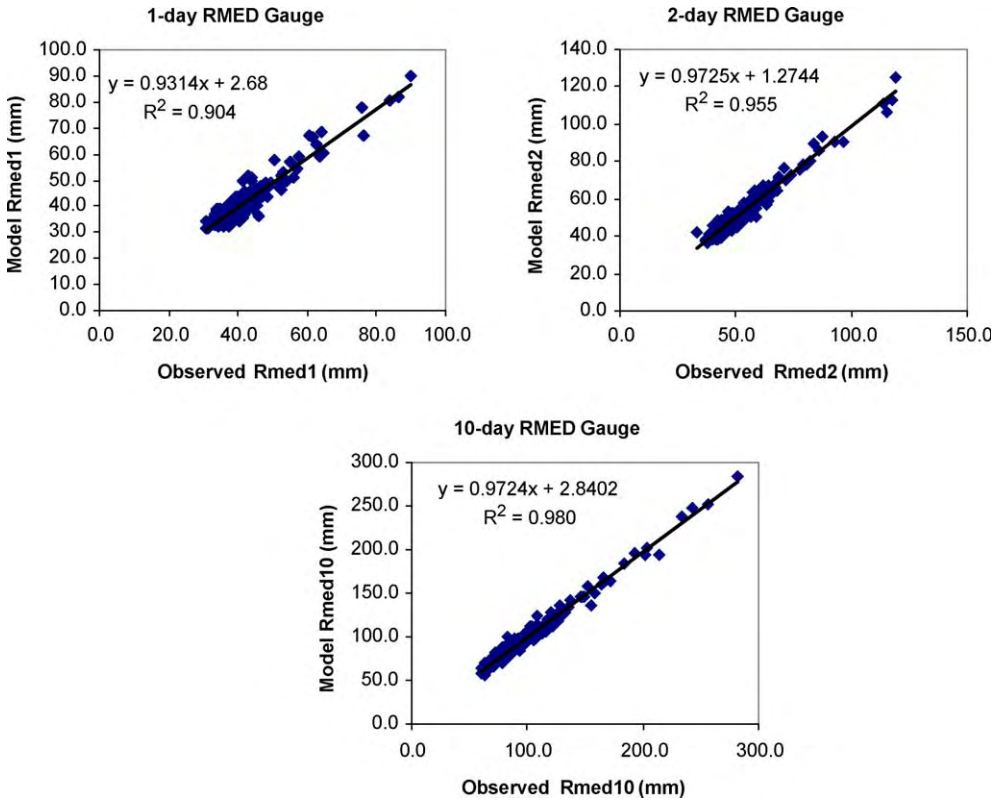

Fig. 3. Rmed values: estimates from regression models vs observed for station data.

the observed values are given in Fig. 3. Inspection of the residuals reveals that sites with the highest residuals are essentially different for the three durations. To investigate any geographic variation in model fitting, the residuals were plotted on maps (not shown) and this showed a slight tendency for model overestimation in the north-west and understimation in the south-east. An improved model may be obtained using Geographically Weighted Regression (Brunsdon et al., 2001) or a similar technique. Finally, 5 km grids of 1-, 2- and 10-day Rmed were calculated from the observed UKMO five-day Rmed grid.

In order to make the regressed 5 km Rmed data comparable to the 50 km HadRM3H model data, Rmed values were averaged within each HadRM3H grid box. To estimate other quantiles the averaged Rmed values were then scaled using coefficients derived from the regional growth curves produced in the RFA.

3.3. Areal reduction factors

It is generally accepted that the grid box rainfall of GCMs have the spatial characteristics of areal averages (Reed, 1986; Osborn and Hulme, 1997). On this basis we assume that the RCM represents a 50 km climate. However, the maximum areal average rainfall rate will always be less than the maximum rate estimated at a point. This difference is usually referred to as the ARF. Due to the differences in scale between the observed and

Table 3
Areal reduction factors used to convert point rainfall to 2500 km^2 areal average rainfall

Duration (days)	Factor
1	0.87
2	0.90
5	0.93
10	0.94

the RCM datasets it is necessary to apply an ARF. An ARF is a value, which can be applied to a point rainfall of a specified duration and return period to give the areal rainfall of the same duration and return period. Applications of this allow direct comparison of return periods estimated for observed and RCM data. In the UK, the values of ARF given in the Flood Studies Report (NERC, 1975) have been widely used in design, and are used in the FEH (IH, 1999). The ARF values used here are taken from the FEH and are found in Table 3. These vary with duration and size of area but are assumed to be invariant with location within the UK and with return period. The former assumption may not apply to future extreme rainfall as the proportions of convective and frontal rainfall and thus the spatial scale of events may change. Osborn (1997) certainly demonstrated that the long-term-mean intensity of areal-mean rainfall and the long-term-mean intensities at points within this area can change by different relative amounts if the spatial scale of rainfall events changes. The latter assumption has also been challenged in research by Stewart (1989) and Allen and Degaetano (2002) where ARFs were found to decrease with return period. However, it was decided to use the same methodology as FEH given that there is no consensus as to the best approach. Therefore, an ARF (see Table 3 for values) was applied to return period magnitudes estimated for the observed datasets to allow a fair comparison with those estimated for the RCM data.

3.4. Uncertainty estimation

An estimate of uncertainty in return period predictions gives some confidence in the use of the growth curve for design purposes Here we use a non-parametric bootstrap simulation method (Efron, 1979) to estimate confidence intervals for the 5-, 10-, 25- and 50-year return period estimates detailed above. If each dataset of annual maximum values is defined as having n data points then, as defined by Efron and Tibshirani (1993), bootstrap simulation samples the original dataset with replacement multiple times to produce multiple independent samples of size n. This approach is also termed resampling and is described below.

If the original dataset is described as

$$x = \{x_1, x_2, \ldots, x_n\} \quad (2)$$

then for each dataset 100 bootstrap samples are generated as

$$x^* = \{x_1^*, x_2^*, \ldots, x_n^*\} \quad (3)$$

where each x_1^* is a random sample (with replacement) from $\{x_1, x_2, \ldots, x_n\}$.

For each bootstrap sample $\{x_1^*, x_2^*, \ldots, x_n^*\}$, the GEV distribution is then fitted and the event magnitudes for 5-, 10-, 25- and 50-year return periods are estimated. The distribution of these 100 estimates of the event magnitude of a given return period allows the construction of the 5th and 95th percentiles for the GEV distribution fitted to each original dataset.

No explicit account has been taken here of the spatial dependence of rainfall events between stations in a given region. It is clear, however, that in both the observed and modelled data some regions are affected by a single storm event, giving rise to large totals at several sites. Hosking and Wallis (1988), however, found that; (a) any bias in quantile estimates is unchanged by the presence of inter-site dependence; (b) regional heterogeneity exerts a stronger effect on the growth curve than inter-site dependence, and, moreover; (c) even when both heterogeneity and inter-site dependence are present, RFA is more accurate than a single site analysis. As a definitive methodology to account for spatial dependence is unavailable, this research relies on the bootstrap simulation method to estimate the likely error. The 5th and 95th percentiles may then be considered as the uncertainty interval for the various return period estimates, although other methods may give larger estimates of uncertainty.

4. Results

4.1. Mean rainfall

Jones and Reid (2001) found that annual UK rainfall totals were over-estimated by the HadRM2 model. This over-estimation occurs particularly at high grid box average elevations (e.g. western Scotland, Lake District and north Wales) and in the East Anglia region. Here, SAAR (Standard Annual Average Rainfall, 1961–1990) from the observed 5 km×5 km UKMO dataset is compared with the mean annual rainfall from the control climate integration of the HadRM3H model (Fig. 4).

The HadRM3H model overestimates mean rainfall in winter and spring months, particularly at high

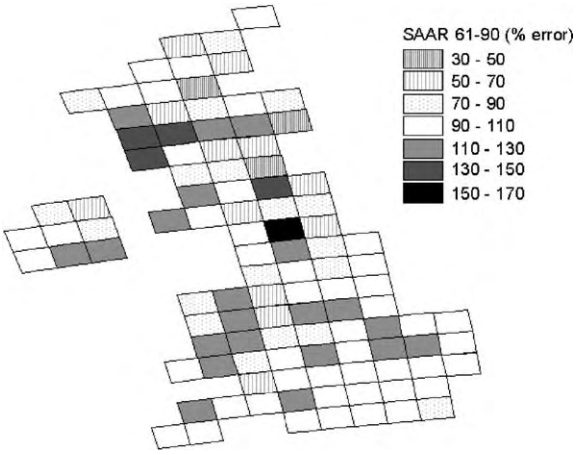

Fig. 4. Percentage errors in representation of mean annual rainfall 1961–1990 by HadRM3H when compared to UKMO dataset.

elevations in a similar way to HadRM2 (Jones and Reid, 2001), but underestimates rainfall in summer and autumn (not shown). These seasonal anomalies lead to a significant underestimation of annual mean rainfall in some parts of the UK (see Fig. 4). This is particularly apparent around eastern coastal regions, and also in the Cheshire plain where, in one of the ensemble members, mean annual rainfall is as low as 250 mm (observed values are between 600 and 700 mm). These discrepancies in model representation of mean annual rainfall are thought to be a result of an over-strong orographic control on rainfall within the HadRM3H model. Not only does this provide a large overestimation of mean annual rainfall in areas of high elevation, but regions on the leeward side of areas of high elevation, such as the north-east England coast, show a classic 'rain-shadow' effect with very low simulated mean annual rainfall.

4.2. Shape of growth curve

The shape of fitted GEV distributions for observed regional AM series was investigated by Fowler and Kilsby (2003a) Although most growth curves were found to approximate a straight line, others had significant curvature. This was found to be especially prevalent in the south of England, and is possibly due to the existence of two mechanisms of extreme rainfall; frontal (flat) and convective (curved upper section) (Fowler and Kilsby, 2003a).

The ratio between the two L-moments L-CV and L-Skewness represents a measure of the shape of the growth curve. Fig. 5 shows a comparison of this ratio for the one-day event for observed and RCM data, respectively. In the observed series, it can be seen that eastern regions generally display a greater L-CV value than western regions, suggesting higher variability in these regions. The highest L-Skewness values are found in southwest and southeast England. These decrease northwards, falling to much lower values in Scotland (Fowler and Kilsby, 2003a). This indicates that rainfall extremes are much larger in the north relative to those in southern regions of the UK. This spatial pattern of variation is similar to those in the Flood Studies Report (NERC, 1975).

Fig. 5 shows that for both RCMs, L-CV and L-Skewness are too low at the one-day level, with the HadRM3H model performing marginally better than the HadRM2 model. However, both modelled series replicate the fall in L-CV from eastern to western regions and in HadRM3H, the observed fall in L-Skewness values from the south to the north of the UK is also replicated. At the 10-day level, HadRM3H again provides an improvement upon HadRM2 (not shown). L-CV and L-Skewness are well represented by HadRM3H in most regions, although there is a slight overestimation of L-Skewness in England.

Fig. 6 shows a comparison of regional growth curves produced for the SEE region using observed, HadRM2 and HadRM3H AM series. The RCM growth curves are too flat, particularly at the one- and two-day level, and underestimate the magnitude of long return period events. The underestimation of the one-day rainfall event magnitude in southeast England by HadRM2 was also noted by Jones and Reid (2001). This may be caused by the poor representation of convective rainfall processes within the RCMs since the one- and two-day AM in these regions tend to be a result of convective summer and autumn storms. Jones and Reid (2001) also attributed this anomaly to the RCM not capturing transient or migratory storm activity arriving from the continent. Further north, one- and two-day AM are generally the result of frontal rainfall in autumn or winter months (see Fig. 7, for example) causing less curvature at the upper end of the growth curve (Fowler and Kilsby, 2003b). RCMs are therefore able

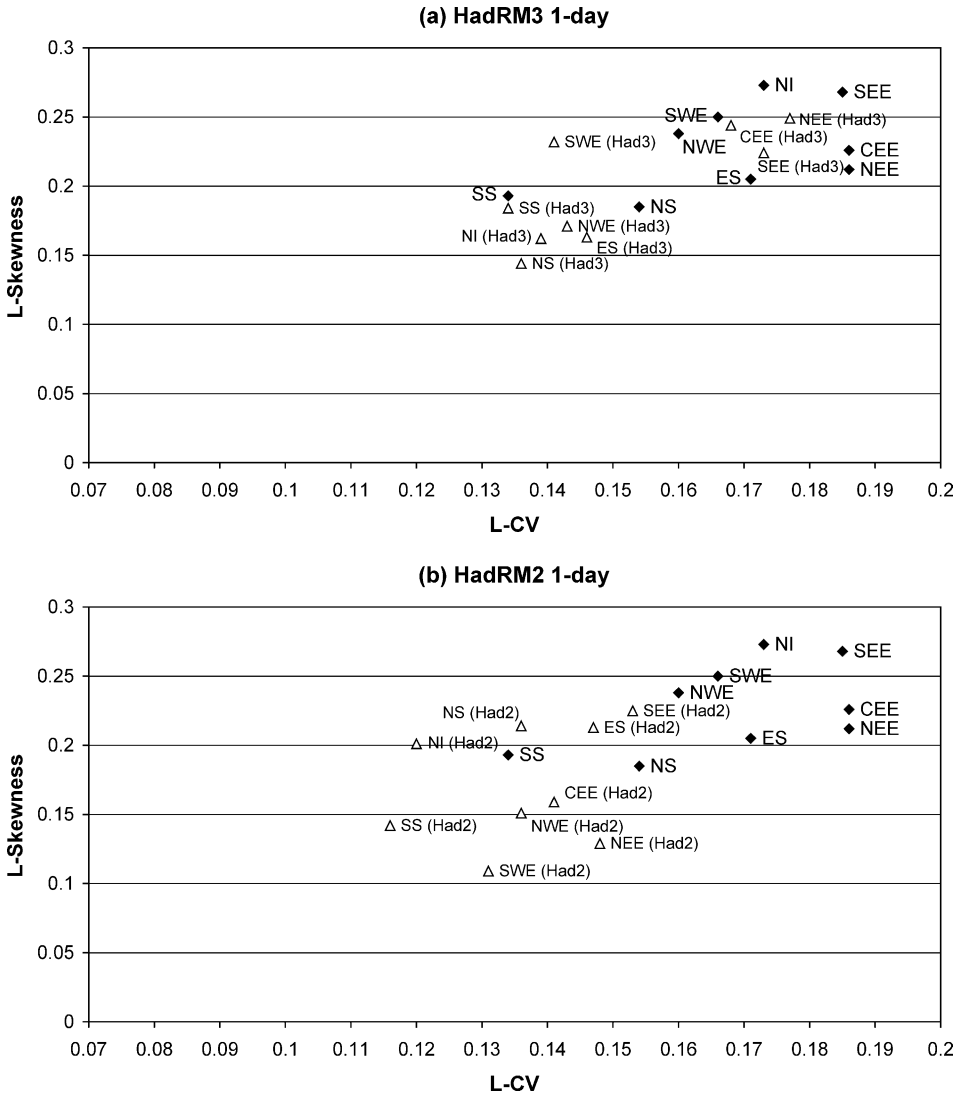

Fig. 5. Comparison of one-day annual maximum observed regional L-CV and L-Skewness with, (a) HadRM3H control ensemble, one-day and, (b) HadRM2 control, one-day.

to simulate extreme one-day AM in these regions better than in more southerly regions of the UK.

4.3. Return period estimates

In this section we use return period (quantile) estimates, firstly to evaluate the representation of extreme rainfall by the RCMs for different regions of the UK and, secondly, to quantify the intra-ensemble variability in the simulation of extreme rainfall events by the HadRM3H model.

4.3.1. Event magnitude of a given return period

Figs. 8–11 present the estimated magnitudes of the 10-year and 50-year return period, using the 1- and 10-day rainfall events for observed, and HadRM2 and HadRM3H control data from the RFA. It can be seen that, in general, magnitudes are lower in the east of England and become higher as a move is made north and west. The event magnitudes at these return periods from the control integrations of both HadRM2 and HadRM3H are quite similar to those from observations. However, it can be seen that both

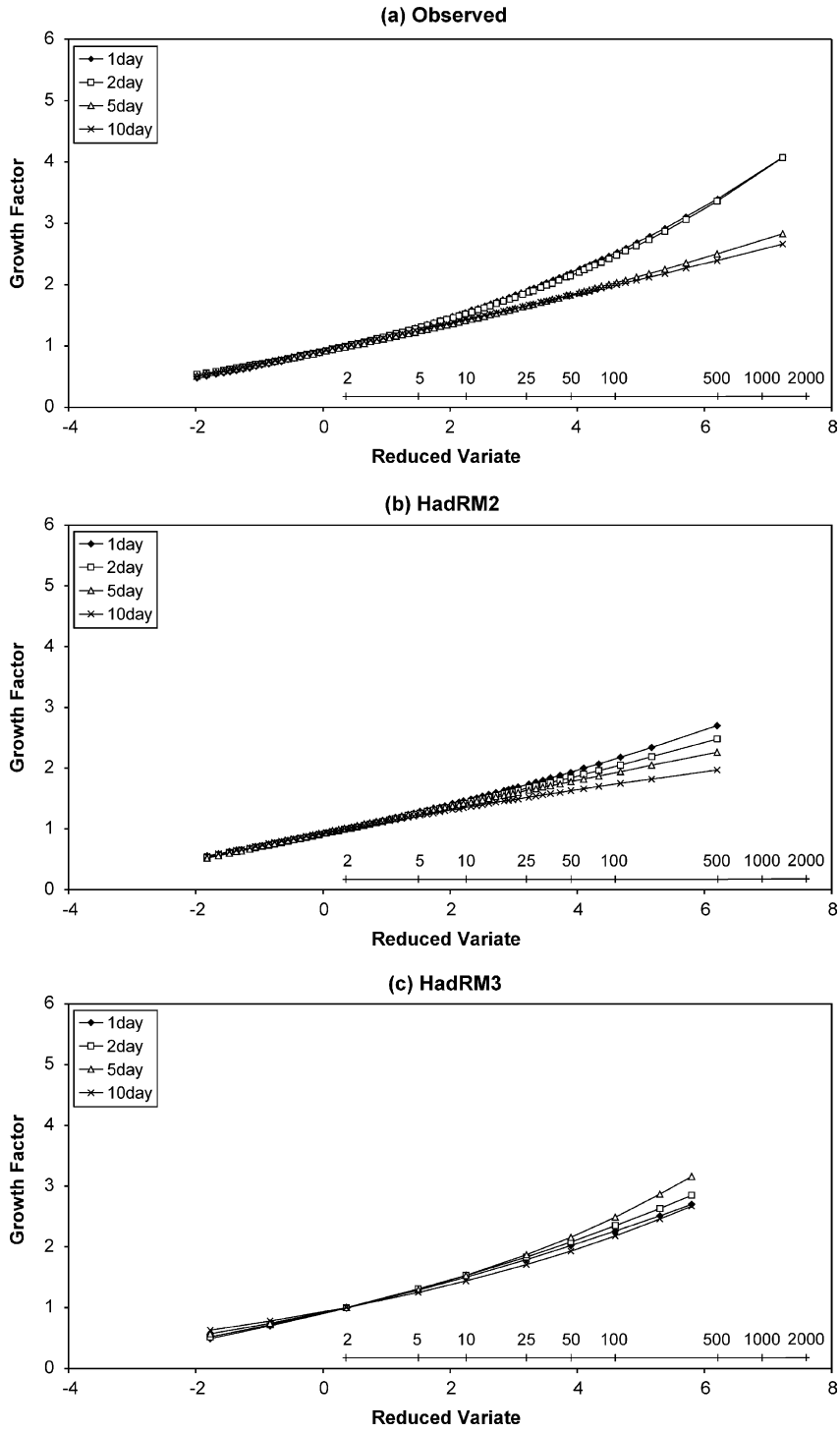

Fig. 6. Comparison of growth curves for southeast England for (a) observed 1961–1990, (b) HadRM2 control climate scenario and, (c) HadRM3H control climate scenario ensemble mean.

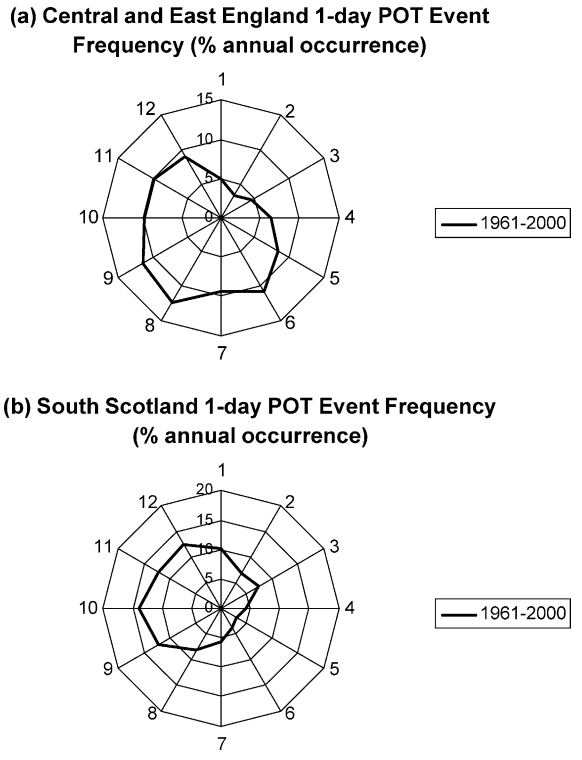

Fig. 7. The timing of extreme rainfall events over parts of the UK from 1961 to 2000, measured using peak-over-threshold analysis. The decadal station frequency of one-day POT events in (a) Central and East England and, (b) South Scotland.

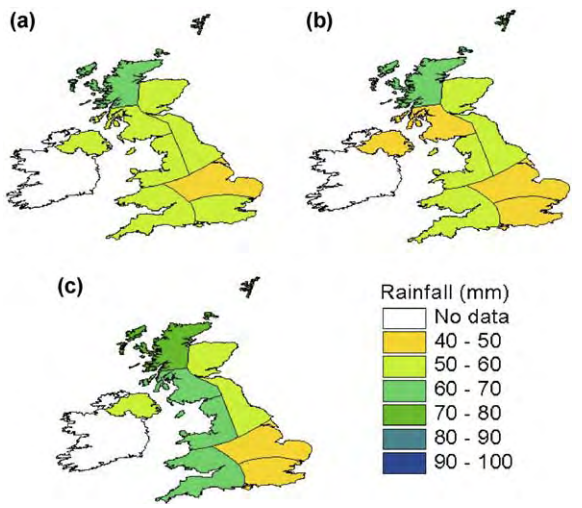

Fig. 8. Comparison of 10-yr, one-day event rainfall magnitudes (mm) for (a) observed, 1961–2000, (b) HadRM2 control and, (c) HadRM3H control.

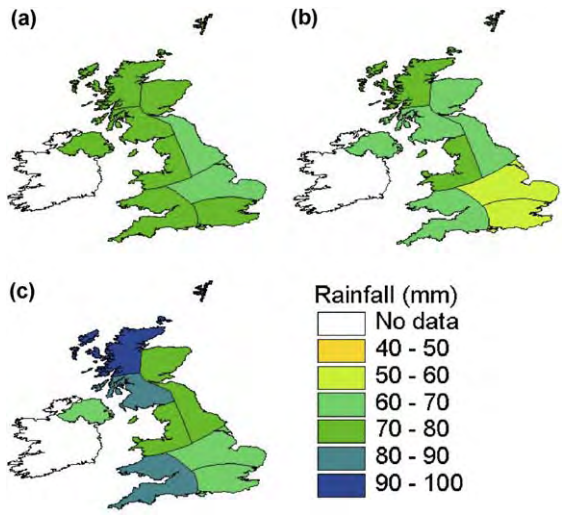

Fig. 9. Comparison of 50-year, one-day event rainfall magnitudes (mm) for (a) observed, 1961–2000, (b) HadRM2 control and, (c) HadRM3H control.

HadRM2 and HadRM3H provide an underestimate of event magnitude in southeast England, with HadRM3H additionally overestimating these in both north Scotland and southwest England. In these regions, the HadRM2 model performs much better than the HadRM3H model in replicating the observed event magnitudes of extreme rainfall, largely as

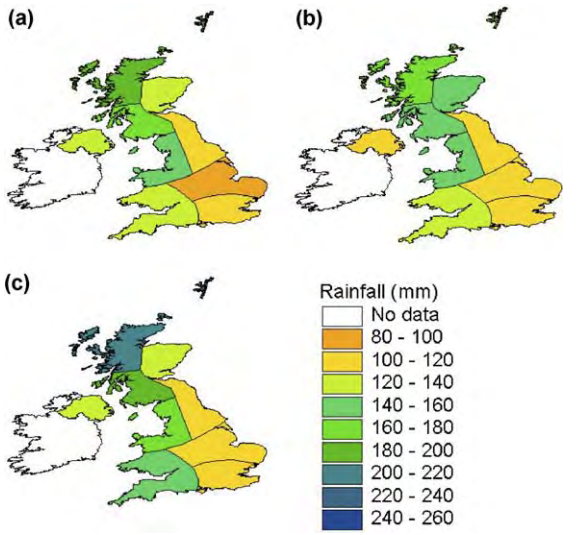

Fig. 10. Comparison of 10-year, 10-day event rainfall magnitudes (mm) for (a) observed, 1961–2000, (b) HadRM2 control and, (c) HadRM3H control.

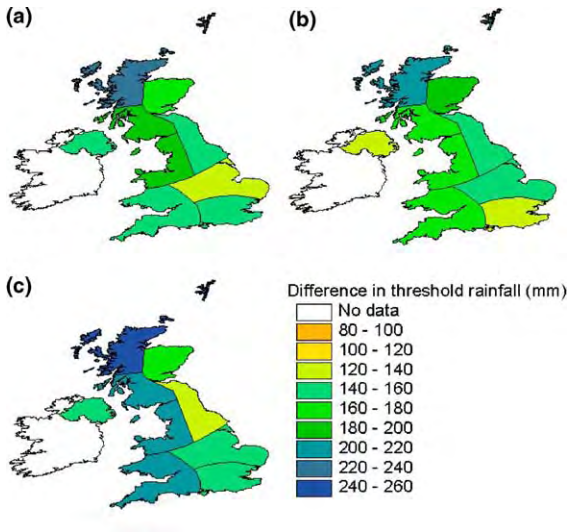

Fig. 11. Comparison of 50-year, 10-day event rainfall magnitudes (mm) for (a) observed, 1961–2000, (b) HadRM2 control and, (c) HadRM3H control.

a result of the better representation of mean rainfall in these regions by the HadRM2 model. However, for both models, the differences between the estimated event magnitude at a given return period for the observed data and control integrations are surprisingly small given the original difference in spatial resolution between the two datasets.

For the three regions of southeast and southwest England and north Scotland more detail is given in Tables 4–6. These show a comparison of the 5-, 10-, 25- and 50-year return period magnitudes for 1-, 2-, 5- and 10-day extreme rainfall events for the observed, and the HadRM2 and HadRM3H control climates. The uncertainty bounds given are taken from the bootstrap simulation method outlined in Section 3.4. Table 4 clearly shows the underestimation of SEE one- and two-day event magnitudes by the HadRM3H and HadRM2 models for higher return period events. This is a consequence of the lack of curvature at the upper end of the growth curve detailed in Section 4.2. In Tables 5 and 6, the event magnitudes for given return periods are shown for the regions of southwest England and north Scotland, respectively. It is likely that the overestimation of event magnitudes in these regions by the HadRM3H model is a direct consequence of the overestimation of mean annual rainfall over high elevation areas (see Section 4.1). This provides a particularly high overestimate over north Scotland.

Differences between the HadRM3H control and the observed event magnitude for a given return period can be better seen using the GBA approach (Fig. 12). There are clear spatial patterns in the HadRM3H estimates, with the largest event magnitudes found

Table 4
The Southeast England region (SEE)-comparison of observed (OBS), HadRM2 and HadRM3H control scenario return period estimates for 1-, 2-, 5- and 10-day duration events

Return period	Dataset	Estimated rainfall (mm)							
		One-day		Two-day		Five-day		Ten-day	
		Min	Max	Min	Max	Min	Max	Min	Max
5 yr	OBS	42	44	51	54	71	74	98	102
	HadRM2	39	40	50	52	71	74	101	104
	HadRM3H	36	37	48	50	67	69	88	91
10 yr	OBS	49	52	60	65	80	85	111	117
	HadRM2	43	46	57	60	80	84	112	117
	HadRM3H	42	44	56	59	79	83	101	106
25 yr	OBS	60	66	74	81	93	101	127	136
	HadRM2	51	54	65	70	91	96	123	130
	HadRM3H	50	53	67	72	95	103	119	127
50 yr	OBS	68	78	85	96	102	113	139	152
	HadRM2	56	61	71	77	98	107	132	142
	HadRM3H	56	60	76	83	109	122	134	145

The observed estimates are adjusted by an areal reduction factor taken from FSR (see Table 3). The uncertainty bounds given here are estimated using the bootstrap simulation method detailed in Section 3.4.

Table 5
The Southwest England region (SWE)-comparison of observed (OBS), HadRM2 and HadRM3H control scenario return period estimates for 1-, 2-, 5- and 10-day duration events

Return period	Dataset	Estimated rainfall (mm)							
		One-day		Two-day		Five-day		Ten-day	
		Min	Max	Min	Max	Min	Max	Min	Max
5 yr	OBS	46	48	59	62	85	88	120	124
	HadRM2	46	48	61	63	88	90	123	126
	HadRM3H	46	47	65	66	94	97	132	135
10 yr	OBS	54	57	68	72	95	99	133	138
	HadRM2	51	53	70	72	100	104	135	140
	HadRM3H	52	54	75	77	107	112	148	153
25 yr	OBS	63	70	80	86	106	113	147	156
	HadRM2	56	59	80	85	118	125	152	160
	HadRM3H	61	64	88	93	125	135	171	179
50 yr	OBS	71	81	89	98	115	124	157	170
	HadRM2	59	64	87	95	133	142	165	176
	HadRM3H	68	73	99	107	140	156	189	201

The observed estimates are adjusted by an areal reduction factor taken from FSR (see Table 3). The uncertainty bounds given here are estimated using the bootstrap simulation method detailed in Section 3.4.

in regions of high elevation, e.g. western Scotland and Wales (not shown). The estimates then decrease eastwards, with the smallest magnitudes found in central England and East Anglia (not shown). This replicates the large observed spatial variation found in regions with complex orography. At longer durations, the spatial variability becomes more pronounced, with the largest spatial variability being found in Scotland which exhibits a pronounced west–east gradient in estimated event magnitude at a given return period between high values in western Scotland and lower values in central and eastern Scotland (not shown).

On average, the HadRM3H model is found to underestimate the event magnitude for a given return

Table 6
The North Scotland region (NS)-comparison of observed (OBS), HadRM2 and HadRM3H control scenario return period estimates for 1-, 2-, 5- and 10-day duration events

Return period	Dataset	Estimated rainfall (mm)							
		One-day		Two-day		Five-day		Ten-day	
		Min	Max	Min	Max	Min	Max	Min	Max
5 yr	OBS	53	54	73	76	112	116	164	169
	HadRM2	53	55	79	82	114	117	158	162
	HadRM3H	59	60	87	90	131	135	184	188
10 yr	OBS	60	63	83	87	125	132	181	188
	HadRM2	60	62	92	95	131	136	175	180
	HadRM3H	66	68	98	101	146	152	202	207
25 yr	OBS	69	74	94	101	142	152	202	214
	HadRM2	69	73	111	116	156	163	196	204
	HadRM3H	73	77	110	115	165	173	222	230
50 yr	OBS	76	82	103	113	154	169	217	234
	HadRM2	76	81	126	132	178	186	214	224
	HadRM3H	79	84	119	126	178	189	235	247

The observed estimates are adjusted by an areal reduction factor taken from FSR (see Table 3). The uncertainty bounds given here are estimated using the bootstrap simulation method detailed in Section 3.4.

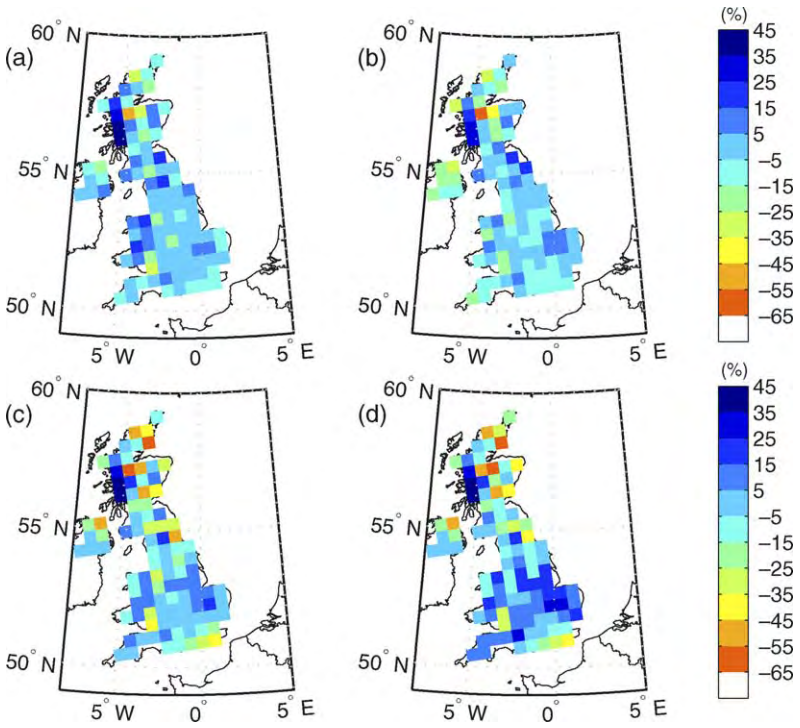

Fig. 12. Difference in return period estimates (%) between the HadRM3H model and the scaled UKMO (HadRM3H/UKMO) data for the one-day event (a) 10-year return period and (b) 50-year return period and the 10-day event (c) 10-year return period and (d) 50-year return period.

period by about 10% for the one-day totals (Fig. 12a and b). However, this is highly spatially variable with anomalies ranging from −50 to +40%. The anomalies between observed and HadRM3H model estimates closely follow the differences in mean rainfall highlighted in Section 4.1. Overall, positive anomalies tend to be associated with increased orography, with the largest model overestimations being found along the west coast of Scotland. The largest underestimations (30–50%) are similarly found in central and eastern Scotland. This suggests that the HadRM3H model largely exaggerates the observed west–east rainfall gradient. For longer duration events, these model differences increase with a range of −80 to +40% for 10-day totals, and significant model underestimation is also found in southeast England (Fig. 12d). This is similar to that found in the regional analysis above and by Jones and Reid (2001) for HadRM2. For the UK as a whole, larger model-observed differences are generally found for higher return period and longer duration events (Fig. 12).

From the range of estimates that are obtained when using the GBA it is clear that some regions exhibit very large variability and the choice of grid box to represent a particular region or case-study within a region may be critical. Table 7 shows, for each region and rainfall duration, the minimum and maximum estimated magnitude of the 5-, 10-, 25- and 50-year return period event. The largest range is found in north and south Scotland (NS and SS). This is closely followed by the west coast of England (SWE and NWE). The smallest regional variability occurs in central England and southeast England (CEE and SEE).

4.3.2. *Uncertainty in estimations*

In this section, we address two kinds of uncertainty. The first relates to HadRM3H, where the three ensemble members provide a measure of the uncertainty in model output or intra-ensemble variability. Secondly, we address the uncertainty in return period estimates using the bootstrap resampling methodology described in Section 3.4. Although limited to the climate variability produced

Table 7
Minimum and maximum HadRM3H return periods estimated using individual GBA per rainfall region

Period (year)	Region	One-day total		Two-day total		Five-day total		Ten-day total	
		Min (mm)	Max (mm)	Min (mm)	Max (mm)	Min (mm)	Max (mm)	Min (mm)	Max (mm)
5	NS	33	114	45	174	58	273	74	387
5	SS	35	102	46	154	66	238	88	336
5	ES	35	59	44	85	60	127	75	170
5	NI	33	49	43	66	58	94	78	130
5	NWE	30	60	39	87	51	126	64	181
5	NEE	31	51	41	70	51	94	63	124
5	CEE	31	41	41	58	57	81	75	109
5	SEE	33	40	44	52	57	76	72	102
5	SWE	33	71	45	104	63	157	85	220
10	NS	38	124	52	192	66	300	82	430
10	SS	40	110	53	168	76	260	100	370
10	ES	40	65	51	96	69	144	85	191
10	NI	38	55	50	74	64	104	86	143
10	NWE	35	67	46	99	61	140	74	200
10	NEE	37	59	49	79	59	106	74	138
10	CEE	36	46	48	66	67	93	88	125
10	SEE	39	46	52	61	68	88	84	115
10	SWE	39	78	53	118	74	178	97	244
25	NS	45	134	61	213	76	330	92	480
25	SS	47	119	61	182	87	284	115	410
25	ES	47	72	59	111	80	164	97	215
25	NI	45	63	58	85	72	118	95	159
25	NWE	42	75	56	113	73	158	88	224
25	NEE	47	71	59	92	72	121	88	154
25	CEE	44	54	57	77	80	112	104	147
25	SEE	48	56	60	73	80	106	101	136
25	SWE	49	86	65	137	91	208	114	274
50	NS	49	141	67	228	83	349	99	515
50	SS	53	124	68	192	95	299	126	437
50	ES	52	77	65	121	89	179	106	233
50	NI	51	68	64	93	77	128	101	171
50	NWE	47	81	64	123	83	172	99	241
50	NEE	52	80	68	100	83	132	100	165
50	CEE	50	60	64	86	92	129	116	165
50	SEE	54	65	67	83	91	125	113	156
50	SWE	57	93	76	152	105	232	126	297

by the three HadRM3H ensemble runs, the resampling of the three sets of AMs in order to calculate multiple sets of return period estimates makes it possible to estimate a confidence interval for the event magnitudes for given return periods that are presented in this study.

Intra-ensemble variability is calculated here as the difference between the lowest and highest ensemble return period estimate (of the three HadRM3H 31-year control ensembles) for each grid box divided by the corresponding return period estimate (using all three ensemble members, i.e. using 93 years). The result may be seen as the proportion of uncertainty in return period estimation relative to the absolute event magnitude at a given return period for each grid box. Since both terms have unit mm the uncertainty measure becomes dimensionless.

Maps of intra-ensemble variability were produced for the daily and all multi-day AM. Here we show maps for only the 1- and 10-day events (Figs. 13 and 14, respectively) to illustrate the spatial differences between HadRM3H model

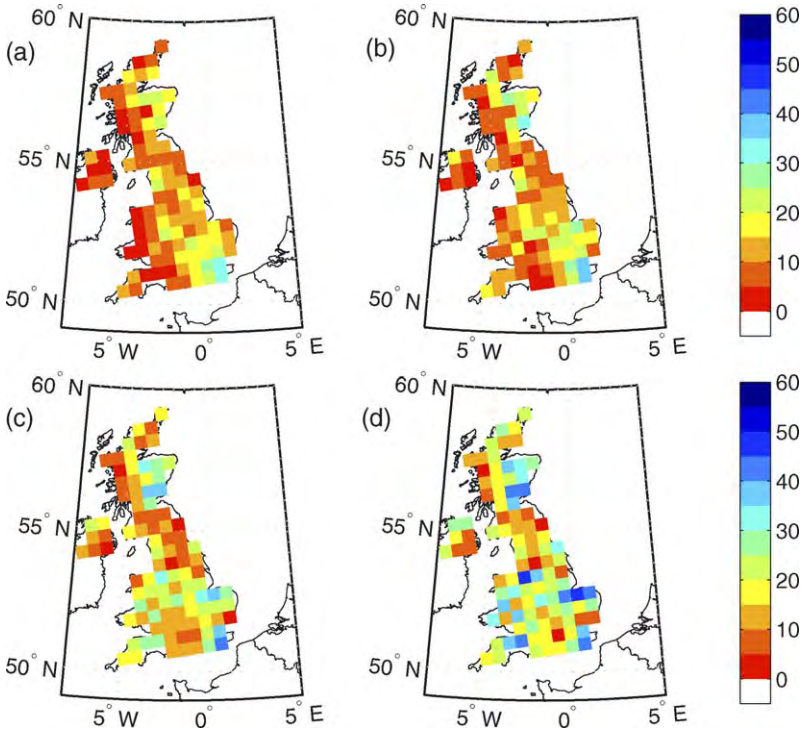

Fig. 13. Proportion of uncertainty range relative to magnitude of the HadRM3H return period estimates for the one-day event, where (a) 5-year return period, (b) 10-year return period, (c) 25-year return period and (d) 50-year return period.

ensemble members. For all rainfall durations (some not shown here) the intra-ensemble variability in event magnitude estimated for a given return period varies from 1 to 50% for the different grid boxes where, generally, higher values are associated with longer return periods. For one-day duration events, at lower return periods the largest variability in estimate is found in eastern regions, particularly southeast England and eastern Scotland (Fig. 13). At longer return periods, most regions show increases in intra-ensemble variability. However, in western Scotland, Northern Ireland and northern England, the intra-ensemble variability appears small. For most grid boxes intra-ensemble variability decreases for longer duration events, the exception being grid boxes over much of Scotland and northern England (Fig. 14).

The uncertainties associated with event magnitude estimates for a given return period are presented as the ratio of the uncertainty range (using the 5th and 95th percentile, as estimated from the bootstrap procedure) to the actual return period estimate. These ratios give an indication of how large the uncertainty is relative to the estimate itself. Results are presented here for the 10- and 50-year return period magnitudes using the 1- and 10-day event (Fig. 15). As for the intra-ensemble uncertainty this measure is also dimensionless. Because of the relatively smaller event magnitudes in east and southeast England, the uncertainty range has a larger effect in these regions than west and northwest regions of the UK. Hence, the spatial pattern shows increasing uncertainty from west to east, and from north to south. The uncertainty ratios are generally of similar magnitude at all durations for the lower return period events. However, uncertainty ratios increase with higher return periods, the increase being somewhat larger for the longer duration events (compare Fig. 15b and d).

5. Discussion and conclusions

We have assessed the performance of a RCM in the simulation of UK extreme rainfall on an annual basis

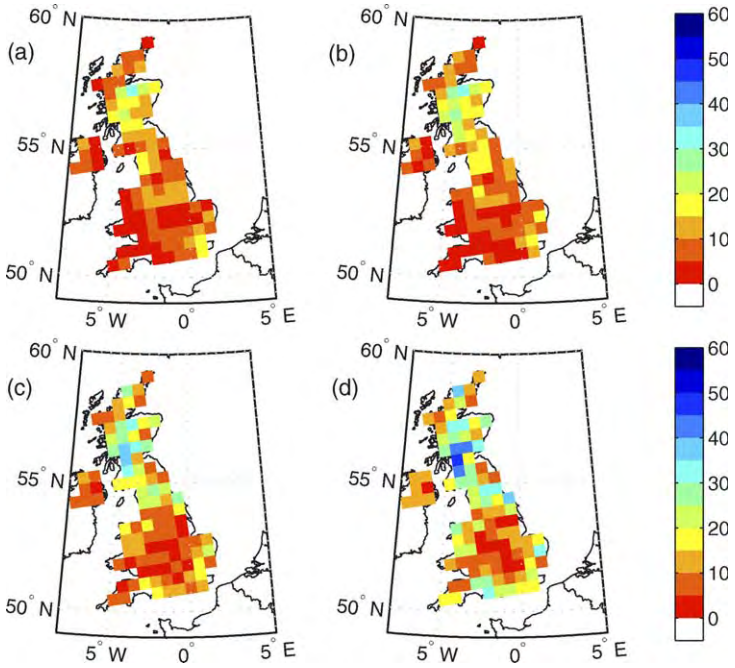

Fig. 14. Proportion of uncertainty range relative to magnitude of return period estimates from HadRM3H for the 10-day event, where (a) 5-year return period, (b) 10-year return period, (c) 25-year return period and (d) 50-year return period.

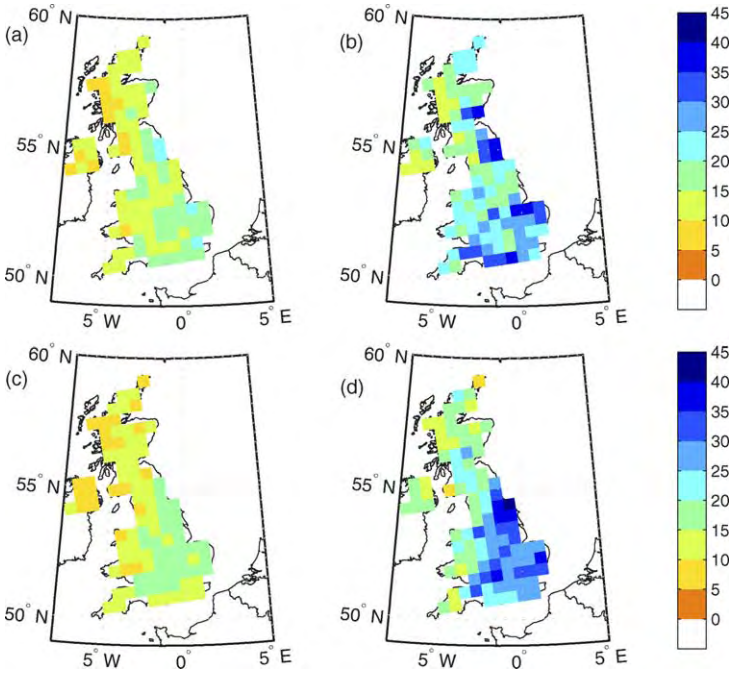

Fig. 15. Uncertainty in return period estimates for the HadRM3H model using the bootstrap simulation method for the one-day event (a) 10-year return period and (b) 50-year return period and the10-day event (c) 10 year-return period and (d) 50-year return period.

using both regional frequency analysis and individual GBA. The major conclusions of this study are:

- HadRM3H overestimates mean annual rainfall in areas of high elevation but in leeward areas there is a classic 'rain shadow' effect with very low simulated mean annual rainfall. This is thought to be a result of an over-strong orographic control within the model, leading to an exaggeration of the observed west–east rainfall gradient.
- However, despite the original differences in spatial resolution between the modelled and observed data, HadRM3H provides a good representation of extreme rainfall at various return periods and durations across most of the UK. Additionally, the GBA shows that HadRM3H is able to replicate the large observed spatial variation in extreme rainfall found in regions with complex orography, particularly for shorter durations.
- In certain regions, particularly north Scotland, there is a large overestimation of extremes. This is thought to be a direct consequence of the estimation of mean rainfall in these regions by HadRM3H, with the largest model overestimations found along the west coast of Scotland.
- Similarly, in eastern 'rain shadowed' regions there is some underestimation of extremes, highlighted particularly by the GBA. The largest underestimations (30–50%) are found in central and east Scotland for one-day rainfall, increasing to about 80% for 10-day rainfalls.
- Significant model underestimation is also found in southern regions of the UK, particularly SEE and SWE. Jones and Reid (2001) attribute this to the lack of model representation of transitory or migratory storm activity from the continent. Here, we attribute this anomaly to the poor representation of convective processes within the model, causing the growth curves to be too flat and underestimating the magnitude of long return period events.

Although there are some problems with the representation of extreme rainfall by the HadRM3H model, almost all are related to the orographic enhancement of mean rainfall. Durman et al. (2001) overcame this for the HadRM2 model by scaling the simulated values to have the same mean as the observations. This allowed the RCM to capture the upper-tail of the rainfall distribution more realistically. However, this methodology relies on the assumption that the scaling will be the same in the future.

It is, therefore, worthwhile considering how best to use the information from this study in informing hydrological design. Whilst it may be desirable to use RCM grid-based data directly and with no modification, it is clear that inaccuracies in the mean climatology and extremes preclude their use in this way. Standard practice for dealing with corrections to a number of climate variables has been to apply factors based on the ratio of the control climatology to observed values on a grid box basis (as Durman et al., 2001). Inspection of the relatively large errors in a number of grid box mean rainfall estimates make this option unattractive even for estimates of mean rainfall, and we would suggest that recourse is made to RFA as demonstrated here. RFA benefits in both the use of more data in extremes estimation, and in averaging to avoid errors from individual grid boxes. Care must, of course, be exercised in cases where the model appears to represent extreme distributions better than the mean. In cases where the spatial pattern is important, then outputs from a grid based analysis will be more appropriate.

Using RFA, the HadRM3H model may be used with some confidence to estimate present extreme rainfall distributions, showing good predictive skill in estimating the statistical properties of extreme rainfall during the baseline period, 1961–1990. This implies that the RCM will also have skill in predicting how these extremes might change under enhanced greenhouse conditions.

Acknowledgements

We thank Tim Osborn (Climatic Research Unit, University of East Anglia, UK) for the use of the daily rainfall data set and the British Atmospheric Data Centre (BADC) for the most recent rainfall data. The HadRM2 and HadRM3H data has been supplied by the Climate Impacts LINK project (DEFRA Contract EPG 1/1/154) on behalf of the Hadley Centre and UK Meteorological Office. The UKMO 5 km datasets were created with financial support from the Department of Environment, Food and Rural Affairs and are being promoted through the UK Climate Impacts Programme (UKCIP). They form part of

the UKCIP02 national climate scenarios prepared for UKCIP by the Tyndall and Hadley Centres. This work is part of the SWURVE (Sustainable Water: Uncertainty, Risk and Vulnerability Estimation in Europe) project, funded under the EU Environment and Sustainable Development programme, grant number EVK1-2000-00075. Richard Jones of the UK Met. Office (Hadley Centre) is thanked for comments on the final draft of this paper. The authors would also like to thank the two anonymous reviewers whose comments helped to improve the paper.

Appendix A. Regional frequency analysis

RFA usually follows a two part *index-flood* procedure, which is a convenient way of pooling statistics from different sample data (Hosking and Wallis, 1997) and can be used for any type of data. If the data are available at N sites, with site i having sample size n_i and observed data X_{ij}, $j=1,\ldots,n$. Then $X_i(F)$, $0<F<1$, forms the frequency distribution's quantile function at site i. In an index-flood procedure, the sites must form a homogeneous region, with identical frequency distributions at the N sites apart from the site-specific scaling factor, the *index-flood* (Hosking and Wallis, 1997).

The index-flood procedure may then be defined as (from Hosking and Wallis, 1997) (Eq. (A1))

$$X_i(F) = \mathrm{Rmed}_i x(F), \quad i = 1,\ldots,N \tag{A1}$$

where Rmed_i is the index-flood (here it is the median of the at-site AM frequency distribution, as in the FEH (IH, 1999)), and $x(F)$ is the regional growth curve, a quantile function identical at every site within that region.

The site-specific *index-flood variable*, Rmed_i, is naturally estimated for each site as the median of the annual maximum dataset at site i.

Secondly, the *regional growth curve*, $x(F)$, $0<F<1$ is derived, using a pooled analysis of the dimensionless rescaled data, $x_{ij}=X_{ij}/Rmed_i$, $j=1,\ldots,n_i$, $I=1,\ldots,N$. Here, L-moments are used to derive the *regional growth curve*. The L-moment ratios of L-CV, L-Skewness and L-Kurtosis are derived for each site within a region and then combined by regional averaging, weighted according to record length (as Hosking and Wallis, 1997). Thus, giving an example formula for L-CV (Eq. (A3))

$$\mathrm{LCV}_{\mathrm{pooled}} = \sum_{i=1}^{N} w_i \mathrm{LCV}_i \tag{A2}$$

where N is the number of sites in the pooling group and the weight w_i is an effective record length at the ith site defined by (Eq. (A3)):

$$w_i = \frac{n_i}{\sum_{i=1}^{N} n_i} \tag{A3}$$

The denominator is the total number of station-years of record in the pooling group, while the numerator is the number of station-years at the ith site. The weighted average L-Skewness and L-Kurtosis moment ratios are derived in the same way.

The usual L-moments approach is then used to fit the GEV (Generalised Extreme Value) distribution for each AM series by matching the sample L-moments to the distribution L-moments.

The GEV distribution has three parameters and is described by (Eq. (A4))

$$x(F) = \xi + \frac{\alpha}{k}(1 - (-\ln F)^k) \quad (k \neq 0) \tag{A4}$$

where ξ is the location parameter, α the scale parameter, k the shape parameter and F refers to a given quantile.

A *regional growth curve* was fitted for each region using the regionally averaged site L-moment ratios. The fitted growth curve is given by (Eq. (A5))

$$x(F) = 1 + \frac{\beta}{k}\{(\ln 2)^k - (-\ln F)^k\}$$

where

$$\beta = \frac{\alpha}{\xi + \frac{\alpha}{k}\{1 - (\ln 2)^k\}} \tag{A5}$$

The parameter k is estimated from the L-skewness (Hosking et al., 1985) (Eq. (A6)):

$$k \approx 7.8590c + 2.9554c^2$$

where

$$c = \frac{2}{3 + t_3} - \frac{\ln 2}{\ln 3} \tag{A6}$$

The parameter β is estimated using L-CV (Hosking and Wallis, 1997) as (Eq. (A7)):

$$\beta = \frac{kt_2}{t_2\{\Gamma(1+k) - (\ln 2)^k\} + \Gamma(1+k)(1-2^{-k})} \quad \text{(A7)}$$

where Γ denotes the gamma function, t_2 is the L-CV L-moment ratio and t_3 is the L-Skewness L-moment ratio.

Quantile estimates at site i can then be obtained by combining the estimates of $Rmed_i$ and $x(F)$ as (Eq. (A8)):

$$X_i(F) = \mathrm{Rmed}_i x(F) \quad \text{(A8)}$$

References

Allen, R.J., Degaetano, A.T., 2002. Re-evaluation of extreme rainfall areal reduction factors American Meteorological Society 13th Conference on Applied Meteorology, May 13th–14th, Oregon 2002.

Brunetti, M., Buffoni, L., Maugeri, M., Nanni, T., 2000. Precipitation intensity trends in northern Italy. International Journal of Climatology 20, 1017–1031.

Brunsdon, C., McClatchey, J., Unwin, D.J., 2001. Spatial variations in the average rainfall-altitude relationship in Great Britain: an approach using geographically weighted regression. International Journal of Climatology 21, 455–466.

Crichton, D., 2002. UK and global insurance responses to flood hazard. Water International 27, 119–131.

DEFRA, 2001. National appraisal of assets at risk from flooding and coastal erosion, including the potential impact of climate change. DEFRA Technical Report.

Durman, C.F., Gregory, J.M., Hassell, D.C., Jones, R.G., Murphy, J.M., 2001. A comparison of extreme European daily precipitation simulated by a global and a regional climate model for present and future climates. Quarterly Journal of the Royal Meteorological Society 127, 1005–1015.

Efron, B., 1979. Bootstrap methods: another look at the jack-knife. Annals of Statistics 7, 1–26.

Efron, B., Tibshirani, R.J., 1993. An Introduction to the Bootstrap. Chapman & Hall, New York. 456 pp.

Ekström, M., Fowler, H.J., Kilsby, C.G., Jones, P.D., 2004. New estimates of future changes in extreme rainfall across the UK using regional climate model integrations. 2. Future estimates and use in impact studies. Journal of Hydrology 2004;.

Fowler, H.J., Kilsby, C.G., 2003a. A regional frequency analysis of United Kingdom extreme rainfall from 1961 to 2000. International Journal of Climatology 23, 1313–1334.

Fowler, H.J., Kilsby, C.G., 2003b. Implications of changes in seasonal and annual extreme rainfall. Geophysical Research Letters 30 (13), 1720 doi: 10.1029/2003GL017327.

Frei, C., Schär, C., 2001. Detection probability of trends in rare events: theory and application to heavy precipitation in the alpine region. Journal of Climate 14, 1568–1584.

Gordon, C., Cooper, C., Senior, C.A., Banks, H., Gregory, J.M., Johns, T.C., Mitchell, J.F.B., Wood, R.A., 2000. The simulation of SST, sea ice extents and ocean heat transports in a version of the Hadley Centre coupled model without flux adjustments. Climate Dynamics 16, 147–168.

Gregory, J.M., Jones, P.D., Wigley, T.M.L., 1991. Precipitation in Britain: an analysis of area-average data updated to 1989. International Journal of Climatology 11, 331–345.

Hennessey, K.J., Gregory, J.M., Mitchell, J.F.B., 1997. Change in daily precipitation under enhanced greenhouse conditions. Climate Dynamics 13, 667–680.

Hosking, J.R.M., Wallis, J.R., 1988. The effect of intersite dependence on regional flood frequency analysis. Water Resources Research 24, 588–600.

Hosking, J.R.M., Wallis, J.R., 1997. Regional Frequency Analysis: An Approach based on L-moments. Cambridge University Press, Cambridge.

Hosking, J.R.M., Wallis, J.R., Wood, E.F., 1985. Estimation of the generalised extreme-value distribution by the method of probability-weighted moments. Technometrics 27, 251–261.

Hulme, M., Jenkins, G.J., Lu, X., Turnpenny, J.R., Mitchell, T.D., Jones, R.G., Lowe, J., Murphy, J.M., Hassell, D., 2002. Climate Change Scenarios for the United Kingdom: the UKCIP02 Scientific Report. Tyndall Centre for Climate Change Research, School of Environmental Sciences, University of East Anglia, Norwich. 120 pp.

Huntingford, C., Jones, R.G., Prudhomme, C., Lamb, R., Gash, J.H.C., Jones, D.A., 2003. Regional climate-model predictions of extreme rainfall for a changing climate. Quarterly Journal of the Royal Meteorological Society 129, 1607–1621.

IH, 1999. Flood Estimation Handbook, 5 volumes. CEH Wallingford (formerly the Institute of Hydrology), Wallingford.

IPCC, 2000. Technical summary, in: Nakicenovic, N., Swart, B. (Eds.), Special Report on Emissions Scenarios. Cambridge University Press, Cambridge. 570 pp.

Iwashima, T., Yamamoto, R., 1993. A statistical analysis of the extreme events: long-term trend of heavy daily precipitation. Journal of the Meteorological Society of Japan 71, 637–640.

Johns, T.C., Carnell, R.E., Crossley, J.F., Mitchell, J.F.B., Senior, C.A., Tett, S.F.B., Wood, R.A., 1997. The second Hadley Centre coupled ocean-atmosphere GCM: model description, spinup and validation. Climate Dynamics 13, 103–134.

Johns, T.C., Gregory, J.M., Ingram, W.J., Johnson, C.E., Jones, A., Lowe, J.A., Mitchell, J.F.B., Roberts, D.L., Sexton, D.M.H., Stevenson, D.S., Tett, S.F.B., Woodage, M.J., 2003. Anthropogenic climate change for 1860 to 2100 simulated with the HadCM3 model under updated emissions scenarios.. Climate Dynamics 20, 583–612.

Jones, P.D., Conway, D., 1997. Precipitation in the British Isles: an analysis of area-average data updated to 1995. International Journal of Climatology 17, 427–438.

Jones, P.D., Reid, P.A., 2001. Assessing future changes in extreme precipitation over Britain using regional climate model integrations. International Journal of Climatology 21, 1337–1356.

Karl, T.R., Knight, R.W., 1998. Secular trends of precipitation amount, frequency and intensity in the United States. Bulletin of the American Meteorological Society 79, 231–241.

Lamb, R., 2001. To what extent can the October/November 200 floods be attributed to climate change DEFRA FD2304 Final Report 2001. 40 pp.

Lawrimore, J.H., Halpert, M.S., Bell, G.D., Menne, M.J., Lyon, B., Schnell, R.C., Gleason, K.L., Easterling, D.R., Thiaw, W., Wright, W.J., Heim, R.R., Robinson, D.A., Alexander, L., 2001. Climate assessment for 2000. Bulletin of the American Meteorological Society 82, S1–S62.

Leggett, J., Pepper, W.J., Swart, R.J., 1992. Emission scenarios for the IPCC: an update, in: Houghton, J.T., Callander, B.A., Varney, S.K. (Eds.), Climate Change 1992: the Supplementary Report to the IPCC Scientific Assessment. Cambridge University Press, Cambridge, pp. 69–95.

Marsh, T.J., 2000. The 2000/2001 floods in the UK: a brief overview. Weather 56, 343–345.

McGuffie, K., Henderson-Sellers, A., Holbrook, N., Kothavala, Z., Balachova, O., Hoekstra, J., 1999. Assessing simulations of daily temperature and precipitation variability with global climate models for present and enhanced greenhouse climates. International Journal of Climatology 19, 1–26.

Mitchell, J.F.B., Johns, T.C., Gregory, J.M., Tett, S.F.B., 1995. Climate response to increasing levels of greenhouse gases and sulphate levels. Nature 376, 501–504.

Murphy, J., 1999. An evaluation of statistical and dynamical techniques for downscaling local climate. Journal of Climate 12, 2256–2284.

Murphy, J., 2000. Predictions of climate change over Europe using statistical and dynamical downscaling techniques. International Journal of Climatology 20, 489–501.

NERC, 1975. Flood Studies Report. Institute of Hydrology, Wallingford.

Osborn, T.J., 1997. Areal and point precipitation intensity changes: implications for the application of climate models. Geophysical Research Letters 24, 2829–2832.

Osborn, T.J., Hulme, M., 1997. Development of a relationship between station and grid-box rainday frequencies for climate model evaluation. Journal of Climate 10, 1885–1908.

Osborn, T.J., Hulme, M., 2002. Evidence for trends in heavy rainfall events over the UK. Philosophical Transactions of the Royal Society, Series A 360, 1313–1325.

Osborn, T.J., Hulme, M., Jones, P.D., Basnett, T.A., 2000. Observed trends in the daily intensity of United Kingdom precipitation. International Journal of Climatology 20, 347–364.

Palmer, T.N., Räisänen, J., 2002. Quantifying the risk of extreme seasonal precipitation events in a changing climate. Nature 415, 512–514.

Palutikof, J.P., Brabson, B.B., Lister, D.H., Adcock, S.T., 1999. A review of methods to calculate extreme wind speeds. Meteorological Applications 6, 119–132.

Pope, V.D., Gallani, M.L., Rowntree, P.R., Stratton, R.A., 2000. The impact of new physical parameterizations in the Hadley Centre climate model: HadAM3. Climate Dynamics 16, 123–146.

Reed, D.N., 1986. Simulation of time series of temperature and precipitation over eastern England by atmospheric general circulation model. Journal of Climatology 6, 233–253.

Stewart, E.J., 1989. Areal reduction factors for design storm construction: joint use of raingauge and radar data. New directions for surface water modeling Proceedings of the Baltimore Symposium, May 1989. IAHS Publication No. 181 1989.

Wigley, T.M.L., Jones, P.D., 1987. England and Wales precipitation: a discussion of recent changes in variability and an update to 1985. Journal of Climatology 7, 231–246.

Wigley, T.M.L., Lough, J.M., Jones, P.D., 1984. Spatial patterns of precipitation in England and Wales and a revised, homogeneous England and Wales precipitation series. Journal of Climatology 4, 1–25.

Zhai, P.M., Sun, A.J., Ren, F.M., Liu, X.N., Gao, B., Zhang, Q., 1999. Chances of climate extremes in China. Climatic Change 42, 203–218.